ChemComm

COMMUNICATION

View Article Online
View Journal | View Issue

Cite this: *Chem. Commun.*, 2021, 57, 8210

Received 7th June 2021,
Accepted 9th July 2021

DOI: 10.1039/d1cc03009d

rsc.li/chemcomm

Dynamics of a [2]rotaxane wheel in a crystalline molecular solid†

Giorgio Baggi,[a] Benjamin H. Wilson,[a] Ayan Dhara,[a] Christopher, A. O'Keefe,‡[a] Robert W. Schurko *[bc] and Stephen J. Loeb *[a]

An H-shaped [2]rotaxane comprising a bis(benzimidazole) axle and a 24-membered crown ether wheel appended with four trityl groups forms a highly crystalline material with enough free volume to allow large amplitude motion of the interlocked macrocycle. Variable-temperature (VT) ^{2}H solid-state nuclear magnetic resonance (SSNMR) was used to characterize the dynamics of the [2]rotaxane wheel in this material.

The relative motions of the individual components of mechanically interlocked molecules (MIMs) (*e.g.*, the axle and wheel of a rotaxane) have given rise to their incorporation in rudimentary molecular machines[1–3] and robots.[4,5] Although MIM dynamics are most often observed in solution,[6,7] recently, their motion has been demonstrated inside the cavities of metal–organic framework (MOF) materials.[8,9] In these studies, the rotation or translation of a mobile and flexible macrocyclic ring has been characterized relative to the rigid framework of the MOF lattice.[10–20] Since porous solids can also be designed using molecular building blocks,[21–24] it was reasoned that it should also be possible to create a crystalline 0D molecular solid using MIMs for which dynamics would be possible in the solid state. To this end, we report herein the preparation and characterisation by variable-temperature (VT) ^{2}H solid-state NMR (SSNMR) spectroscopy, the motion of a large macrocyclic wheel about a rigid axle of a [2]rotaxane in a crystalline molecular solid.

The design of crystalline molecular materials that contain dynamic components is not new. Garcia-Garibay pioneered the concept of amphidynamic crystals[25] – an emergent class of condensed phase matter designed with a combination of lattice-forming elements linked to components that display engineered dynamics in the solid state – some years ago and has demonstrated (among others) that ultra-fast rotors[26,27] (*via* single-bond rotations) can be made to operate in the solid-state using individual molecules as building blocks. Taking a page from the amphidynamic materials playbook, we have re-designed our rigid H-shaped, rotationally active, bis(benzimidazole) [2]rotaxane[28,29] to incorporate four trityl groups. It was rationalised that in the solid state, the resulting edge-to-face interactions of the peripheral trityl groups – a phenyl embrace[30–32] – would create a highly crystalline material with the free volume and stability necessary to allow mobility of the central macrocyclic wheel.

Scheme 1 shows the preparation of the targeted H-shaped [2]rotaxane **2⊂24C6**. The four trityl groups were added to the tetra-bromo precursor **1** using a standard Suzuki coupling procedure to create the naked axle **2**. The macrocycle was then added around the axle to make [2]rotaxane **2⊂24C6** utilising a clipping protocol, which featured ring-closing metathesis (RCM) followed by reduction of the residual double bond using D_2 to incorporate deuterium labels for subsequent ^{2}H SSNMR experiments.

The axle, **2**, and [2]rotaxane, **2⊂24C6**, were characterised by ^{1}H NMR studies, high-resolution mass spectrometry (HR-MS) and single-crystal X-ray diffraction (SCXRD). Fig. 1 shows both ball-and-stick and space-filling representations of the solid-state structure of axle **2** (**UWCM-15**). It is interesting to note that the free volume around the bis(benzimidazole) core of the naked axle is filled by molecules of CH_2Cl_2 rather than being occupied by groups from an adjacent molecule, *i.e.*, the trityl group packing interactions dominate leaving free volume at the core.[33] Fig. 2 shows both ball-and-stick and space-filling representations of the solid-state structure of [2]rotaxane **2⊂24C6** (**UWDM-15**). In this crystalline material, there are no trapped molecules of solvent and the free volume at the bis(benzimidazole) core of the axle is occupied by the interlocked **24C6** macrocycle rather than CH_2Cl_2 molecules.

[a] *Department of Chemistry and Biochemistry, University of Windsor, Windsor, ON N9B 3P4, Canada. E-mail: loeb@uwindsor.ca*
[b] *Department of Chemistry and Biochemistry, Florida State University, Tallahassee, FL, 32306, USA*
[c] *National High Magnetic Field Laboratory, Tallahassee, FL 32310, USA*

† Electronic supplementary information (ESI) available: Details of [2]rotaxane synthesis and characterization including full set of VT ^{2}H SSNMR spectra. CCDC 2079257 and 2079258. For ESI and crystallographic data in CIF or other electronic format see DOI: 10.1039/d1cc03009d

‡ Current address: Department of Chemistry, University of Cambridge, Lensfield Road, Cambridge, CB2 1EW, UK.

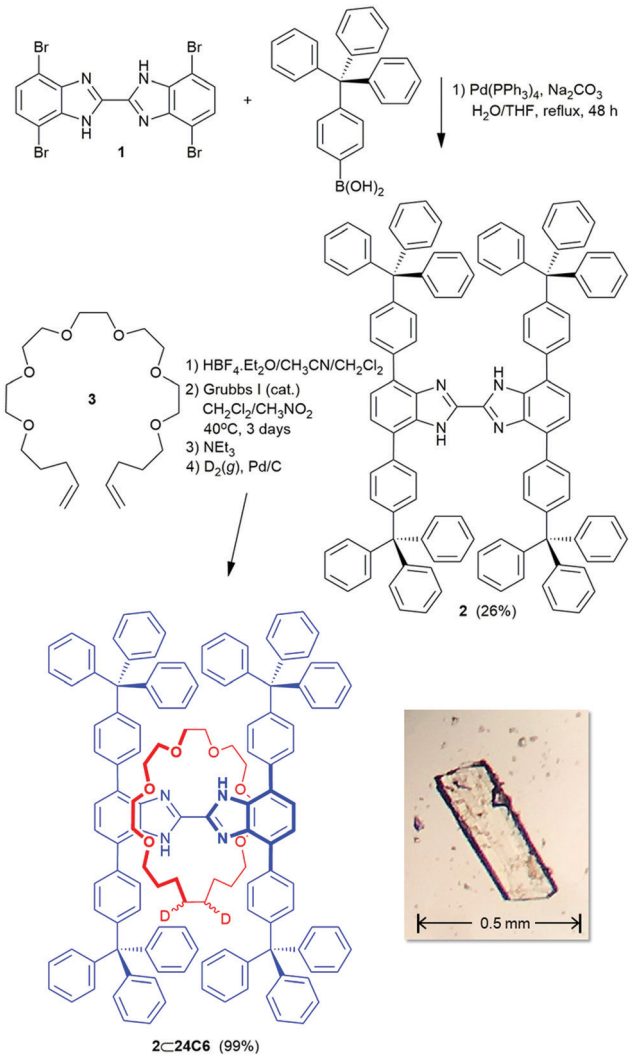

Scheme 1 Preparation of axle **2** and [2]rotaxane **2⊂24C6**.

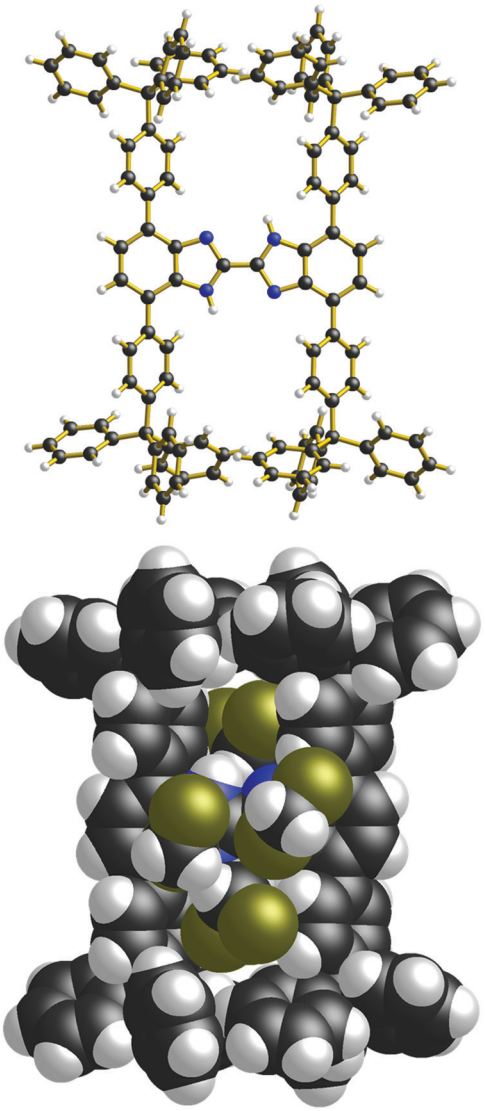

Fig. 1 Single-crystal X-ray structure (170 K) of axle **2**. Top a ball-and-stick representation with solvent molecules omitted for clarity. Bottom a space-filling representation showing CH_2Cl_2 solvent molecules occupying the free volume around the core of the bis(benzimidazole) axle.

Fig. 3a shows a comparison of experimental and simulated PXRD for **2⊂24C6**, verifying that the bulk material is the same highly crystalline material used for SCXRD analysis. The crystals of **2** easily desolvate, losing CH_2Cl_2 rapidly upon removal from the mother liquor; however, crystalline **2⊂24C6** is quite robust by comparison. Fig. 3b shows the TGA of bulk crystalline **2⊂24C6** showing excellent stability to over 300 °C (MP: decomp. >350 °C dec.; see ESI† for details of TGA, DSC and VT PXRD measurements).

VT ^{2}H SSNMR shows that the **24C6** macrocycle is free to undergo dynamic motion very similar to that observed when the same macrocycle is attached to the rigid [2]rotaxane framework in a MOF (*i.e.*, in the **UWDM** series).[12,15–17] Selected experimental ^{2}H SSNMR spectra are shown in Fig. 4a with accompanying simulated spectra in Fig. 4b (see ESI,† Fig. S11 for full set of experimental VT ^{2}H SSNMR spectra). The static spectrum acquired at 185 K was simulated with quadrupolar parameters C_Q = 165(5) kHz and η_Q = 0.0. At this temperature, any motions that are occurring are with rates in the slow-motion limit (SML) and are too slow to influence the appearance of the powder pattern (Fig. 4c). Increasing the temperature results in a change in the appearance of the pattern which is attributed to the onset of a two-site jump motion of the CD_2 groups about an axis that is colinear with the C–C bond that connects the two groups (Fig. 4d). The spectrum acquired at 276 K was simulated with a two-site jump through an angle of 65° with rates in the fast-motion limit (FML, *i.e.*, $\nu_{ex} > 10^7$ Hz). Powder patterns near 276 K lack the sharp discontinuous features observed at lower and higher temperatures, perhaps indicating a range of different motional rates (Fig. S11, ESI†). Increasing the temperature further results in a narrowing of the pattern and the spectrum acquired at 411 K was simulated with a two-site jump through an angle of 70° combined with partial rotation of the ring with rates in the FML. In the partial rotation model, the crown ether ring rotates through 225° in steps of 45° such that the hydrogen-bond donor on the axle interacts with each of the six oxygen atoms on the ring

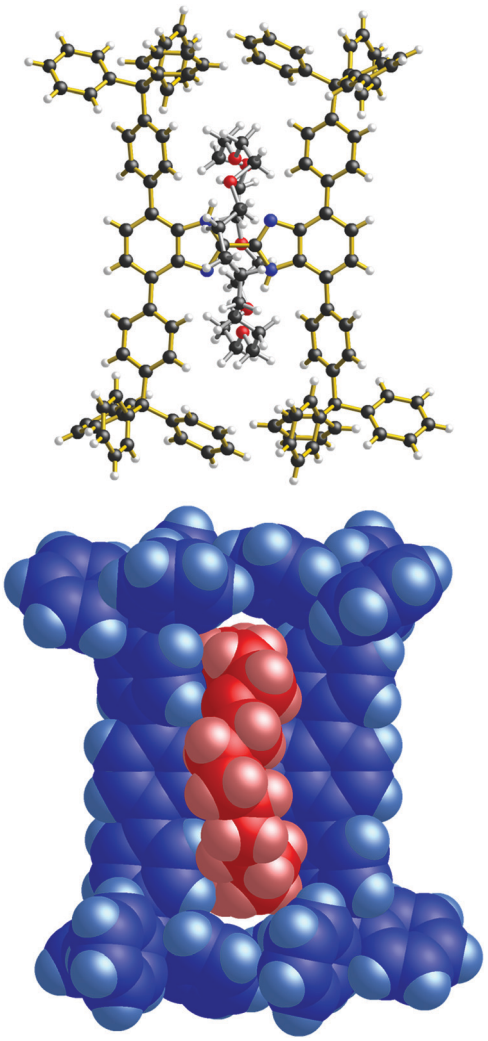

Fig. 2 Single-crystal X-ray structure (170 K) of [2]rotaxane **2⊂24C6**. Top a ball-and-stick representation. Bottom a space-filling representation showing how the macrocyclic **24C6** wheel occupies the free volume around the core of the bis(benzimidazole) axle that was filled by CH_2Cl_2 solvent molecules in the structure of **2**.

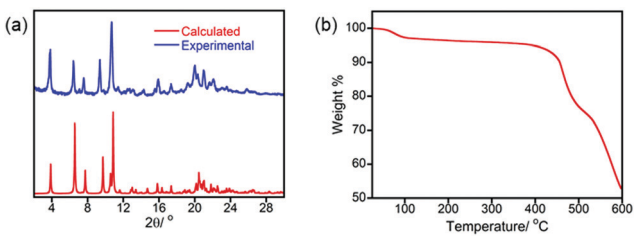

Fig. 3 (a) Experimental and simulated (from single-crystal X-ray diffraction data) PXRD for [2]rotaxane **2⊂24C6**. (b) TGA for [2]rotaxane **2⊂24C6**.

(Fig. 4e). Finally, the spectrum acquired at 479 K was simulated with a model consisting of a two-site jump combined with full rotation of the ring (Fig. 4f), similar to that used in the description of the motion in the pillared MOF **β-UWDM-3**.[12] Here, jumps between the oxygen atom positions occur with rates in the FML and jumps

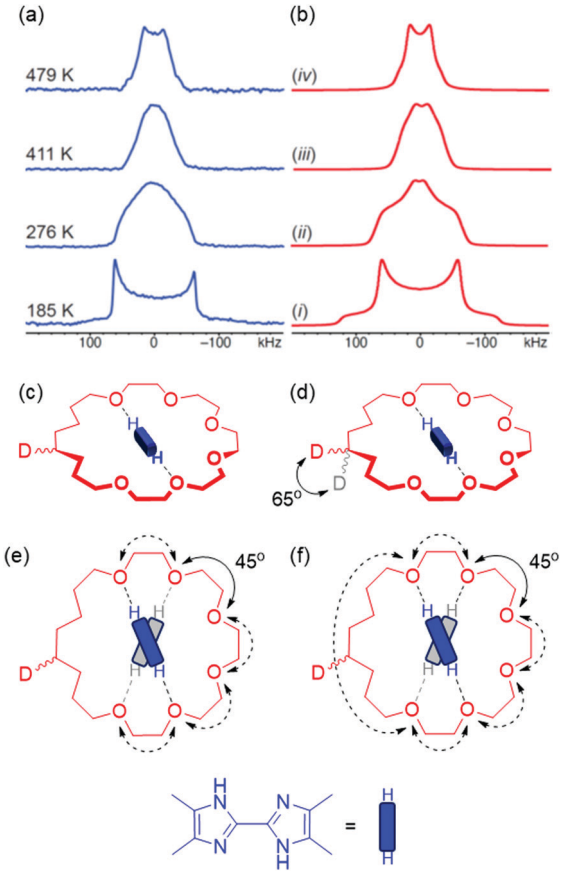

Fig. 4 (a) Experimental ^{2}H VT SSNMR powder patterns (blue) and (b) corresponding analytical simulations (red) for **2⊂24C6** where motions are (i) occurring at rates within the SML and do not affect the appearance of the powder pattern, (ii) two-site jumps through an angle of 65°, (iii) two-site jumps through 70° combined with partial rotation of the ring in 45° steps through 225°, and (iv) two-site jumps through 70° combined with full, rapid rotation of the ring. Schematic representations of the possible modes of motion of the macrocyclic rings within the **2⊂24C6**, including (c) no motion of the macrocyclic ring, (d) two-site jump of the CD_2 groups, (e) partial rotation of the macrocycle about the six ether oxygen atoms within the ring, in addition to the two-site jump of the CD_2 groups, (f) full rotation of the macrocyclic ring, in addition to the two-site jump of the CD_2 groups.

through the alkyl portion of the ring occur at a rate of 10^6 Hz (*i.e.*, ten times slower).

This study demonstrates that the fundamental concepts of crystal engineering – building blocks and intermolecular interactions – can be adapted to create a thermally robust 0D molecular material with sufficient free volume to allow rotation of the wheel of a [2]rotaxane about its axle in the solid state. In particular, trityl groups (crystal engineering synthons) were attached to an H-shaped axle to provide a rigid framework onto which a flexible, and potentially mobile wheel could be trapped *via* a mechanical bond. VT ^{2}H SSNMR was then used to show that the motions – conformational changes, partial rotation, and full rotation – of the interlocked macrocycle are very similar to those observed when a similar molecular system is part of a MOF material. These results suggest that it should be

possible to create molecular solids with MIMs such as switchable catenanes and molecular shuttles by using suitably designed building blocks such as the trityl groups featured in this work.

Conceptualization, S. J. L. and G. B.; synthesis, G. B. and A. D.; materials characterisation, A. D. and B. H. W.; investigation – SSNMR; C. A. O.; formal analysis – SSNMR, C. A. O. and R. W. S.; writing – original draft, B. H. W. and S. J. L.; writing – review & editing, S. J. L., R. W. S., C. A. O., and B. H. W.; funding acquisition, S. J. L. and R. W. S.

S. J. L. acknowledges the Natural Sciences and Engineering Research Council of Canada for support of a Discovery Grant (RGPIN-2018_101694) and a Canada Research Chair. R. W. S. is grateful for research support from The Florida State University and the National High Magnetic Field Laboratory (NHMFL), which is funded by the National Science Foundation Cooperative Agreement (DMR-1644779) and by the State of Florida. R. W. S. also thanks the University of Windsor, the Canadian Foundation for Innovation, and the Ontario Innovation Trust for support of the solid-state NMR facilities at Windsor, and Natural Sciences and Engineering Research Council for a Discovery Grant (RGPIN-2016_06642).

Conflicts of interest

There are no conflicts to declare.

Notes and references

1 S. Erbas-Cakmak, D. A. Leigh, C. T. McTernan and A. L. Nussbaumer, *Chem. Rev.*, 2015, **115**, 10081–10206.
2 E. R. Kay, D. A. Leigh and F. Zerbetto, *Angew. Chem., Int. Ed.*, 2007, **46**, 72–191.
3 S. Kassem, T. van Leeuwen, A. S. Lubbe, M. R. Wilson, B. L. Feringa and D. A. Leigh, *Chem. Soc. Rev.*, 2017, **46**, 2592–2621.
4 S. Kassem, A. T. L. Lee, D. A. Leigh, V. Marcos, L. I. Palmer and S. Pisano, *Nature*, 2017, **549**, 374–378.
5 B. Lewandowski, G. De Bo, J. W. Ward, M. Papmeyer, S. Kuschel, M. J. Aldegunde, P. M. E. Gramlich, D. Heckmann, S. M. Goldup, D. M. D'Souza, A. E. Fernandes and D. A. Leigh, *Science*, 2013, **339**, 189.
6 D. Xia, P. Wei, B. Shia and F. Huang, *Chem. Commun.*, 2016, **52**, 513–516.
7 M. Xue, Y. Yang, X. Chi, X. Yan and F. Huang, *Chem. Rev.*, 2015, **115**, 7398–7501.
8 P. Martinez-Bulit, A. J. Stirk and S. J. Loeb, *Trends Chem.*, 2019, **1**, 588–600.
9 B. H. Wilson and S. J. Loeb, *Chem.*, 2020, **6**, 1604–1612.
10 B. H. Wilson, C. S. Vojvodin, G. Gholami, L. M. Abdulla, C. A. O'Keefe, R. W. Schurko and S. J. Loeb, *Chem.*, 2021, **7**, 202–211.
11 K. Zhu, C. A. O'Keefe, V. N. Vukotic, R. W. Schurko and S. J. Loeb, *Nat. Chem.*, 2015, **7**, 514–519.
12 K. Zhu, V. N. Vukotic, C. A. O'Keefe, R. W. Schurko and S. J. Loeb, *J. Am. Chem. Soc.*, 2014, **136**, 7403–7409.
13 B. H. Wilson, L. M. Abdulla, R. W. Schurko and S. J. Loeb, *Chem. Sci.*, 2021, **12**, 3944–3951.
14 G. Gholami, B. H. Wilson, K. Zhu, C. A. O'Keefe, R. W. Schurko and S. J. Loeb, *Faraday Discuss.*, 2021, **225**, 358–370.
15 V. N. Vukotic, C. A. O'Keefe, K. Zhu, K. J. Harris, C. To, R. W. Schurko and S. J. Loeb, *J. Am. Chem. Soc.*, 2015, **137**, 9643–9651.
16 V. N. Vukotic, K. J. Harris, K. Zhu, R. W. Schurko and S. J. Loeb, *Nat. Chem.*, 2012, **4**, 456–460.
17 P. Martinez-Bulit, C. A. O'Keefe, K. Zhu, R. W. Schurko and S. J. Loeb, *Cryst. Growth Des.*, 2019, **19**, 5679–5685.
18 A. J. Stirk, B. H. Wilson, C. A. O'Keefe, H. Amarne, K. Zhu, R. W. Schurko and S. J. Loeb, *Nano Res.*, 2021, **14**, 417–422.
19 A. Saura-Sanmartin, A. Martinez-Cuezva, D. Bautista, M. R. B. Marzari, M. A. P. Martins, M. Alajarin and J. Berna, *J. Am. Chem. Soc.*, 2020, **142**, 13442–13449.
20 Q. Chen, J. Sun, P. Li, I. Hod, P. Z. Moghadam, Z. S. Kean, R. Q. Snurr, J. T. Hupp, O. K. Farha and J. F. Stoddart, *J. Am. Chem. Soc.*, 2016, **138**, 14242–14245.
21 A. G. Slater and A. I. Cooper, *Science*, 2015, **348**, 8075–8085.
22 P. S. Nugent, V. L. Rhodus, T. Pham, K. Forrest, L. Wojtas, B. Space and M. J. Zaworotko, *J. Am. Chem. Soc.*, 2013, **135**, 10950–10953.
23 B. H. Wilson, H. S. Scott, O. T. Qazvini, S. G. Telfer, C. Mathonière, R. Clérac and P. E. Kruger, *Chem. Commun.*, 2018, **54**, 13391–13394.
24 M. A. Little and A. I. Cooper, *Adv. Funct. Mater.*, 2020, **30**, 1909842.
25 S. D. Karlen and M. A. Garcia-Garibay, Amphidynamic Crystals: Structural Blueprints for Molecular Machines, in *Molecular Machines*, ed. T. R. Kelly, Springer Berlin Heidelberg, Berlin, Heidelberg, 2005; pp. 179–227.
26 A. Colin-Molina, D. P. Karothu, M. J. Jellen, R. A. Toscano, M. A. Garcia-Garibay, P. Naumov and B. Rodríguez-Molina, *Matter*, 2019, **1**, 1033–1046.
27 C. S. Vogelsberg, F. J. Uribe-Romo, A. S. Lipton, S. Yang, K. N. Houk, S. Brown and M. A. Garcia-Garibay, *Proc. Natl. Acad. Sci. U. S. A.*, 2017, **114**, 13613.
28 G. Baggi and S. J. Loeb, *Angew. Chem., Int. Ed.*, 2016, **55**, 12533–12537.
29 G. Baggi and S. J. Loeb, *Chem. – Eur. J.*, 2017, **23**, 14163–14166.
30 A. Duong, A. Lévesque, C. Homand, T. Maris and J. D. Wuest, *J. Org. Chem.*, 2020, **85**, 4026–4035.
31 I. Dance and M. Scudder, *CrystEngComm*, 2009, **11**, 2233–2247.
32 I. Dance and M. Scudder, *Chem. – Eur. J.*, 1996, **2**, 481–486.
33 S. D. Karlen, S. I. Khan and M. A. Garcia-Garibay, *Mol. Cryst. Liq. Cryst.*, 2006, **456**, 221–230.